

Supporting Information for

**Enhanced Photoelectrochemical Water Oxidation Performance
of Fe₂O₃ Nanorods Array by S Doping**

Rong Zhang,[†] Yiyu Fang,[‡] Tao Chen,[†] Fengli Qu,[§] Zhiang Liu,[§] Gu

Du,^{||} Abdullah M. Asiri,[∫] Tao Gao,^{‡,*} and Xuping Sun^{†,*}

[†]College of Chemistry and [‡]Institute of Atomic and Molecular Physics, Sichuan University, Chengdu 610064, China, [§]Chemistry and Chemical Engineering, Qufu Normal University, Qufu 273165, Shandong, China, ^{||}Chengdu Institute of Geology and Mineral Resources, Chengdu 610064, China, and [∫]Chemistry Department, Faculty of Science, King Abdulaziz University, Jeddah 21589, Saudi Arabia

E-mail: gaotao@scu.edu.cn (T.G.); sunxp@scu.edu.cn (X.S.)

Content

Experimental Section

XPS spectrum.....	Figure S1
XPS valence band spectra.....	Figure S2
Tauc plots.....	Figure S3
Energy diagram.....	Figure S4
UV-visible absorption spectra.....	Figure S5
LSV curves.....	Figure S6
LSV curves.....	Figure S7
LSV curves.....	Figure S8
DOS.....	Figure S9
Band structures.....	Figure S10
Electron density distribution plots.....	Figure S11
Comparison of PEC performance.....	Table S1
Electron effective mass.....	Table S2

Experimental Section

Materials: $\text{FeCl}_3 \cdot 6\text{H}_2\text{O}$, NaOH, sulfur powder, H_2O_2 and urea were purchased from Aladdin Ltd. in Shanghai. Ti plate was provided by Hongshan District, Wuhan Instrument Surgical Instruments business, and was pretreated in HCl and then cleaned by sonication in water and ethanol for several times to remove surface impurities. The water used throughout all experiments was purified through a Millipore system.

Preparation of Fe_2O_3 and S: Fe_2O_3 on Ti plate: $\text{FeCl}_3 \cdot 6\text{H}_2\text{O}$ (0.81g) and urea (0.18g) were dissolved in 40 mL water under vigorous stirring for 30 min. Then the solution was transferred to a 50 mL Teflon-lined stainless-steel autoclave in which a piece of Ti plate was immersed into the solution. Then the autoclave was sealed and maintained at 100 °C for 10 h in an electric oven. After the autoclave cooled down at room temperature naturally, the Ti plate covered with Fe-precursor was taken out and washed with water and ethanol for several times, followed by drying at 60 °C. Then the Fe-precursor was annealed at 550 °C in air for 2 h to obtain the Fe_2O_3 nanorods array. To synthesize S: Fe_2O_3 , Fe-precursor on Ti plate and S powder (0.15g) were put at two separate positions in a porcelain boat with S powder at the upstream side of the furnace. The center of the furnace was elevated to 400 °C at a ramping rate of 5 °C min^{-1} and held at this temperature for 20 min in air, and then naturally cooled to ambient temperature in air.

Characterizations: XRD measurements were performed using a RigakuD/MAX 2550 diffractometer with Cu $K\alpha$ radiation ($\lambda = 1.5418 \text{ \AA}$). SEM images were collected on a XL30 ESEM FEG scanning electron microscope at an accelerating voltage of 20

kV. TEM measurements were made on a HITACHI H-8100 electron microscopy (Hitachi, Tokyo, Japan) with an accelerating voltage of 200 kV. XPS measurements were performed on an ESCALABMK II X-ray photoelectron spectrometer using Mg as the exciting source. ICP-MS analysis was performed on ThermoScientific iCAP6300. The diffuse reflectance UV-visible adsorption spectra were recorded on a spectrophotometer (Shimadazu, UV 3600), with fine BaSO₄ powder as reference.

Photoelectrochemical measurements: Photoelectrochemical measurements were performed with a CHI 660E electrochemical analyzer (CH Instruments, Inc., Shanghai) in a standard three-electrode system using Fe₂O₃/Ti or Se-Fe₂O₃/Ti as the working electrode, Pt wire as the counter electrode, and Ag/AgCl as the reference electrode in 1.0 M NaOH. Lighting apparatus used in the experiment is simulated solar light irradiation (100 mW cm⁻²) (PLS-sxe300/300UV). The potentials reported in this work were calibrated to RHE other than especially explained, using the following equation: $E(\text{RHE}) = E(\text{Ag/AgCl}) + (0.197 + 0.059 \times \text{pH}) \text{ V}$. Polarization curves were obtained by linear sweep voltammetry with a scan rate of 5 mV s⁻¹. All experiments were carried out at room temperature. IPCE measurements were performed under illumination through monochromatic system, composed of a monochromator (Model: 74125, Newport) and light source (Model 73404, Newport) without external bias in a two-electrode model, with Fe₂O₃/Ti or Se-Fe₂O₃/Ti as the anode and Pt wire as the cathode. The electrochemical impedance spectroscopy (EIS) was measured using a PGSTAT 302N Autolab Potentiostat/Galvanostat (Metrohm) equipped with a frequency-analyzer module (FRA2) with an excitation signal of 10

mV amplitude and frequency range between 100 kHz to 0.1 Hz.

The applied bias photon-to-current efficiency (ABPE) is calculated based on the equation:

$$ABPE = \frac{j_{ph}(1.23 - V_b)}{P_{total}}$$

where V_b is the applied bias vs. RHE, j_{ph} is the photocurrent density at the measured potential, and P_{total} is the power density of incident light (100 mW cm^{-2}).

The IPCE of each sample was measured in 1.0 M NaOH at 1.23 V vs. RHE under monochromatic illumination, which is calculated based on the equation:

$$IPCE(\%) = \frac{1240 I}{\lambda J_{light}} \times 100\%$$

where I is photocurrent density (mA cm^{-2}), J_{light} is incident light irradiance (mW cm^{-2}), and λ is incident light wavelength (nm).

Mott-Schottky measurements were performed at a frequency of 1000 Hz under dark condition in 1.0 M NaOH. The calculation is based on the equation:

$$\frac{1}{C^2} = \frac{2}{N_D e \epsilon \epsilon_0} \left[(E_S - E_{FB}) - \frac{k_B T}{e} \right]$$

where C is the space charge capacitance of the semiconductor, ϵ is the dielectric constant of Fe_2O_3 , ϵ_0 is the permittivity of vacuum, A is the active area of the photoanode, e is the electronic charge, N_D is the charge carrier concentration, E is the applied potential, E_{fb} is the flat band potential, k_B is Boltzmann's constant, and T is the absolute temperature. The charge carrier density is calculated based on the equation:

$$N_D = -\left(\frac{2}{e\epsilon\epsilon_0}\right)\left(\frac{d\left(\frac{1}{C^2}\right)}{d(E_S)}\right)^{-1}$$

The charge separation efficiency (η_{sep}) and surface transfer efficiency (η_{trans}) is calculated based on the equation:

$$\eta_{\text{trans}} = \frac{J_{\text{H}_2\text{O}}}{J_{\text{H}_2\text{O}_2}}$$

$$\eta_{\text{sep}} = \frac{J_{\text{H}_2\text{O}_2}}{J_{\text{max}} \times \eta_{\text{abs}}}$$

Where $J_{\text{H}_2\text{O}}$ is the measured photocurrent density, $J_{\text{H}_2\text{O}_2}$ is the photocurrent density in the presence of H_2O_2 , J_{max} is the maximum theoretical water oxidation photocurrent density, η_{abs} is the light absorption efficiency.

The band gap is estimated by the equation $(\alpha h\nu)^n = A(h\nu - E_g)$, where $h\nu$ is the incident photon energy, α is the absorption coefficient, and A is a constant. The value of n is 1/2 for hematite.

DFT calculations: all the calculations were based on the projected augmented wave (PAW) formalism of DFT+U as implemented in the Vienna Ab-initio Simulation Package (VASP). The generalized gradient approximation (GGA) method with Perdew-Burke-Ernzerhof (PBE) for the exchange-correlation energy was used. A plane-wave basis set with a kinetic energy cutoff of 400eV is used. The convergence for energy between two consecutive steps was 1.0×10^{-4} eV atom⁻¹ and structure optimizations were performed until the Hellmann-Feynman force on each atom was less than 0.01 eV Å⁻¹. The valence band orbital is the O 2p while the conduction band orbitals are Fe 3d and 4s. The Brillouin zone integrations were performed by using

Gamma-centered Monkhorst-Pack scheme with $5 \times 5 \times 1$ k-points and a Gaussian smearing of 0.1 eV.

The equation of the electron effective mass is :

$$m = \frac{1}{\frac{1}{\hbar^2} \frac{d^2 E}{dk^2}}$$

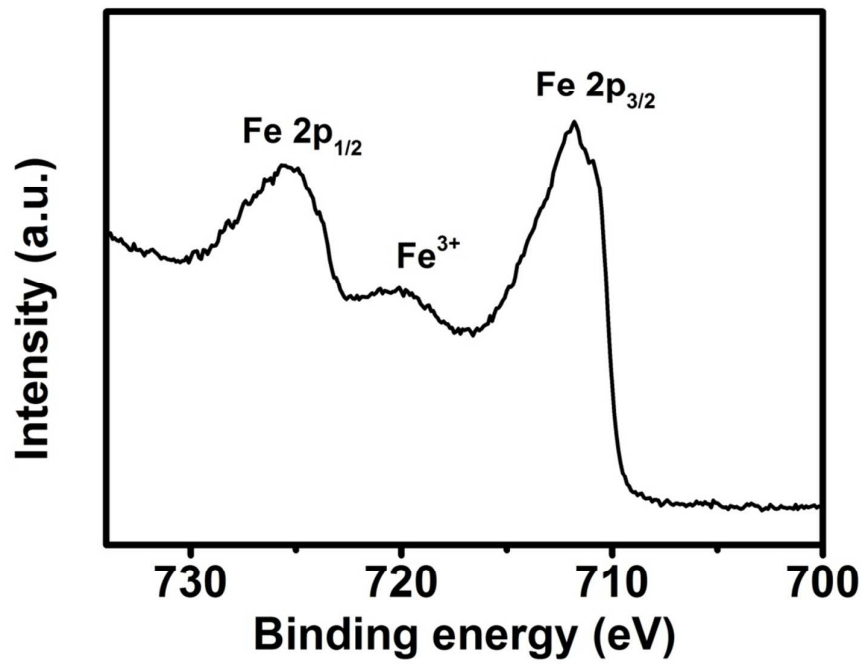


Figure S1. XPS spectrum of Fe₂O₃ in Fe 2p region.

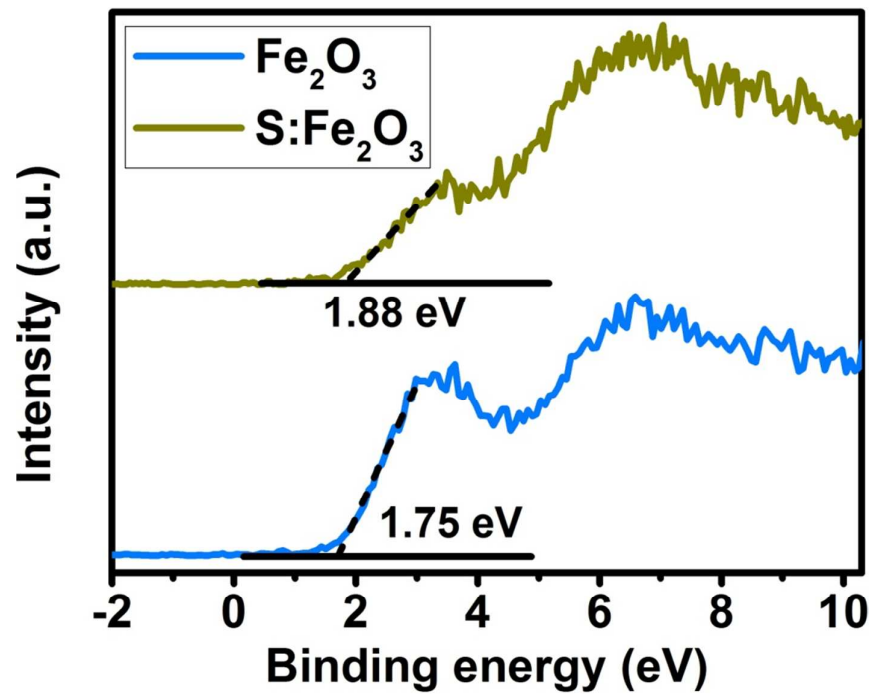


Figure S2. XPS valence band spectra of Fe_2O_3 and $\text{S:Fe}_2\text{O}_3$.

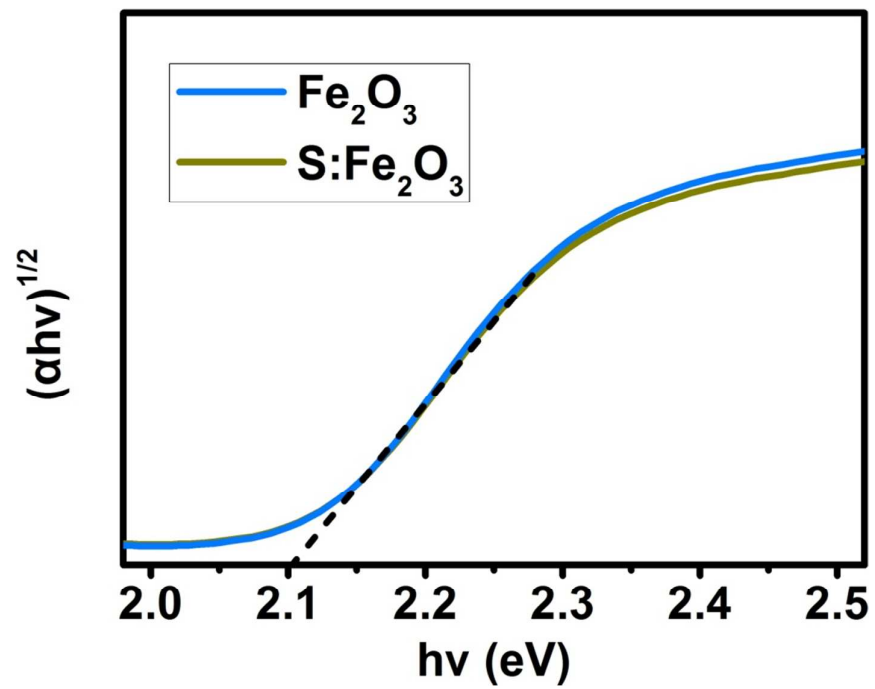


Figure S3. Tauc plots of Fe_2O_3 and $\text{S}:\text{Fe}_2\text{O}_3$.

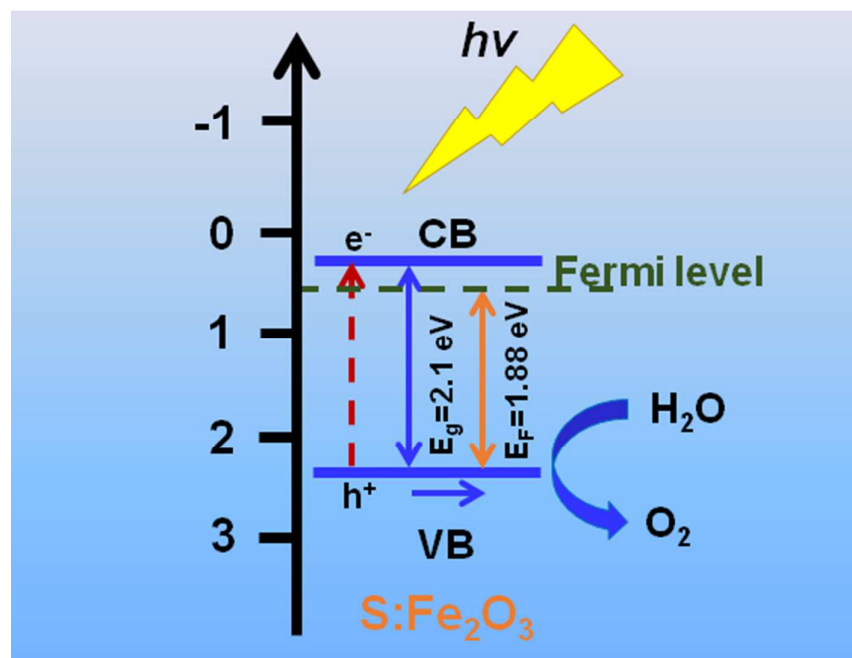


Figure S4. Energy diagram of Fe₂O₃ and S:Fe₂O₃.

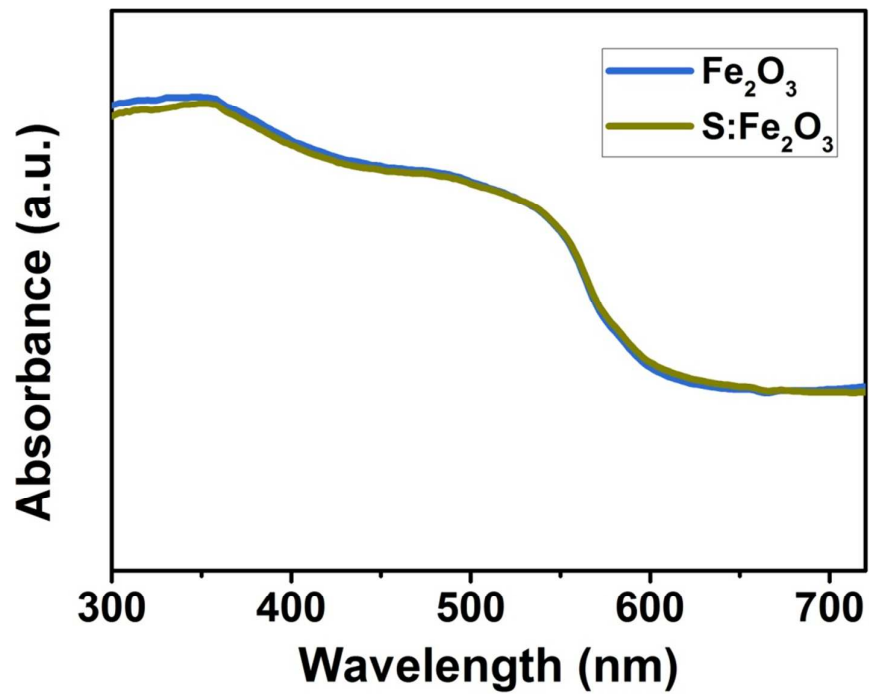


Figure S5. UV-visible absorption spectra of Fe₂O₃ and S:Fe₂O₃.

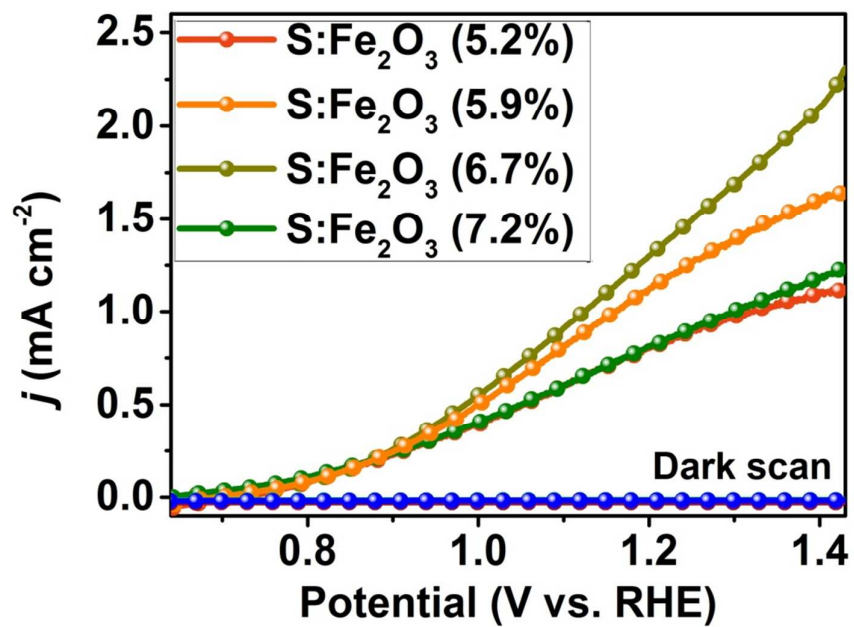


Figure S6. LSV curves of S:Fe₂O₃ with different doping degree.

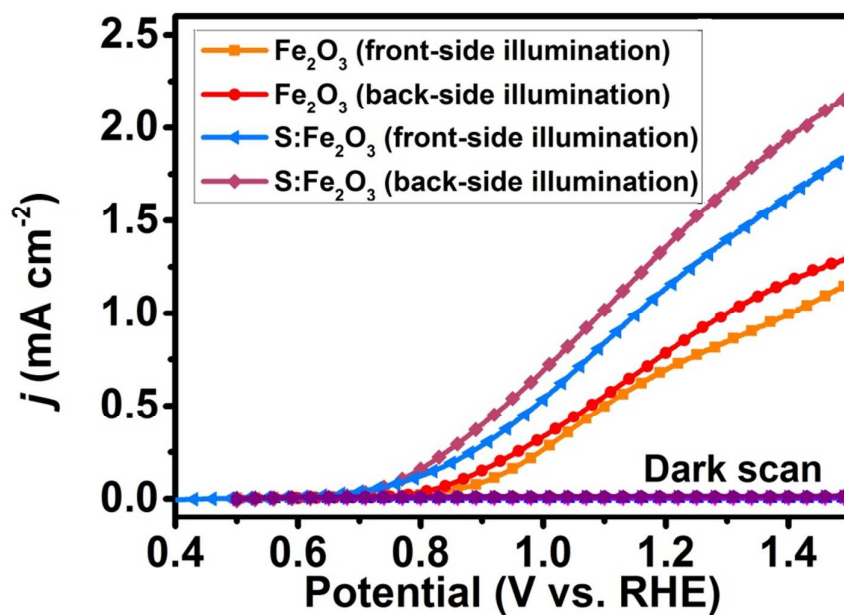


Figure S7. LSV curves of S-doped Fe₂O₃ on FTO in 1.0 M NaOH in the dark and under back- and front-side illumination

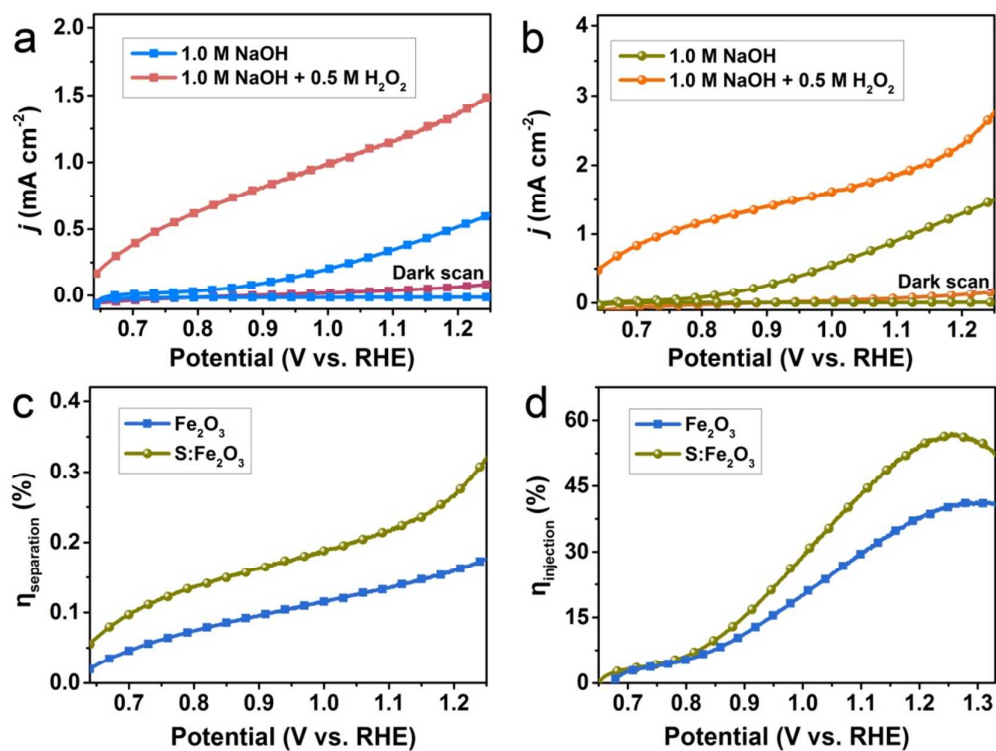


Figure S8. LSV curves for (a) Fe₂O₃ and (b) S:Fe₂O₃ on Ti plate in the dark and under AM 1.5G illumination in 1.0 M NaOH and 1.0 M NaOH + 0.5 M H₂O₂ electrolytes. (c) $\eta_{\text{separation}}$ and (d) $\eta_{\text{injection}}$ of Fe₂O₃ and S:Fe₂O₃.

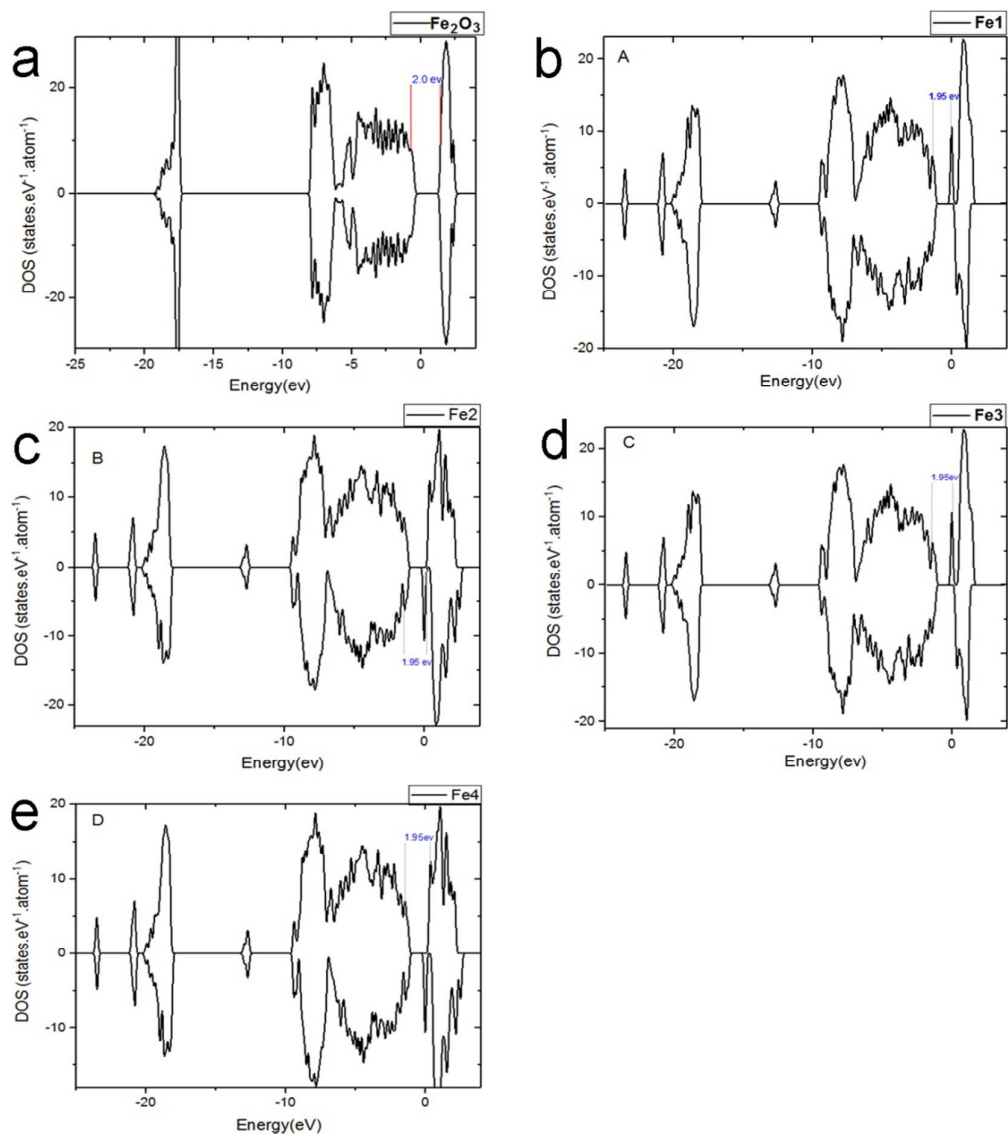


Figure S9. DOS of (a) Fe_2O_3 and (b-e) S-doped Fe_2O_3 .

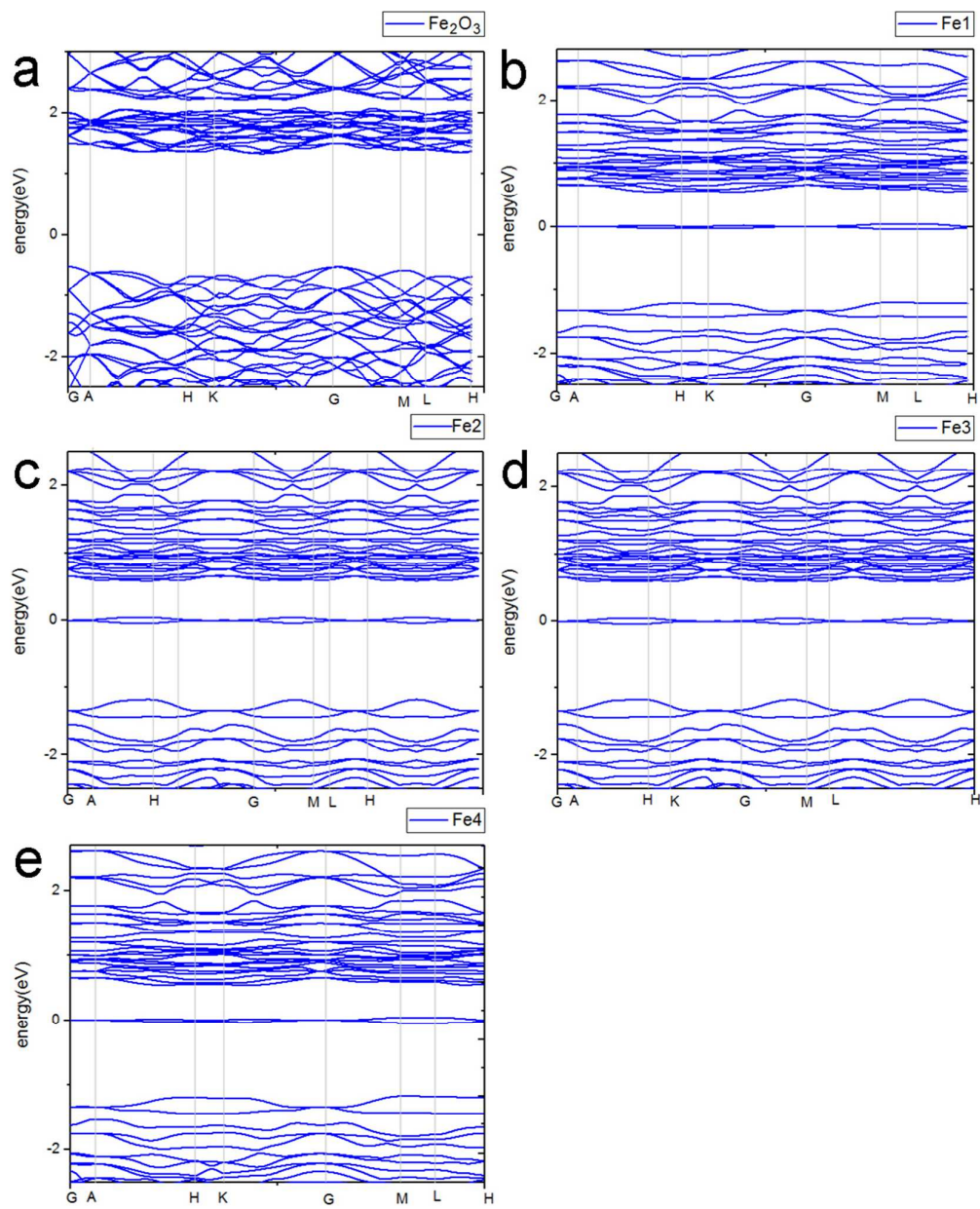


Figure S10. Band structures of (a) Fe_2O_3 and (b-e) S-doped Fe_2O_3 .

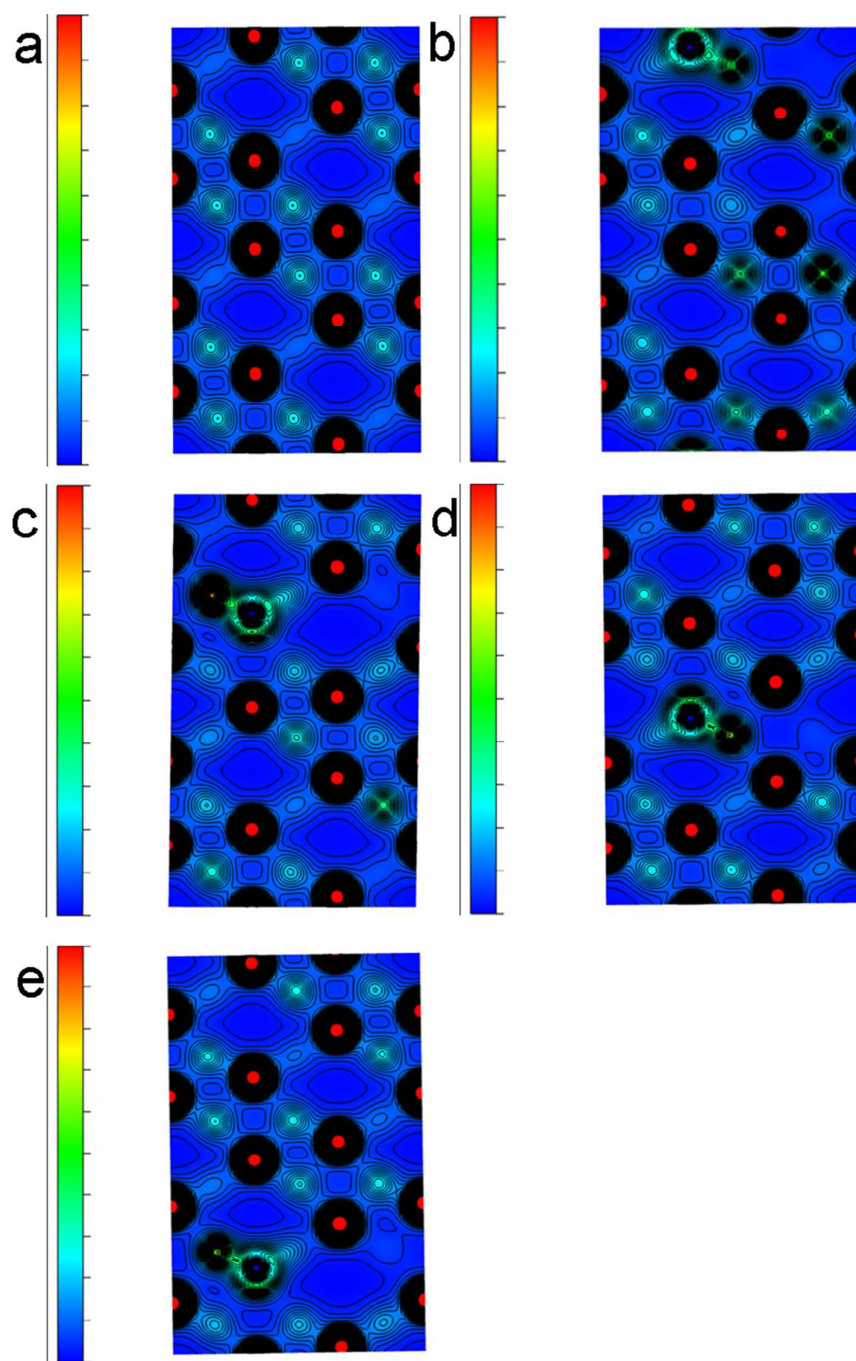


Figure S11. Electron density distribution plots for (a) Fe₂O₃ and (b-e) S-doped Fe₂O₃.

(110) surface.

Table S1. Comparison of Fe₂O₃ and doped Fe₂O₃ photoanodes in PEC system.

Photoanode	Potential (V vs. RHE)	<i>j</i> (mA cm ⁻²)	Ref.
Se-Fe ₂ O ₃	1.23	1.44	<i>This work</i>
Sn,Zr-Fe ₂ O ₃	1.23	1.34	1
Mn:Fe ₂ O ₃	1.23	1.60	2
Fe ₂ O ₃	1.23	0.50	
Si doped α -Fe ₂ O ₃	1.23	1.45	3
La doped hematite	1.23	0.11	4
Ti doped hematite	1.23	0.42	5
Sn-doped α -Fe ₂ O ₃	1.23	1.00	6
Grad-P:Fe ₂ O ₃	1.23	1.48	7
Fe ₂ O ₃	1.23	0.58	
Pt-doped α -Fe ₂ O ₃	1.23	~0.70	8
Ge-doped α -Fe ₂ O ₃	1.23	1.40	9
Hematite on ATO	~1.668	0.67	10

Table S2. Electron effective mass calculated for Fe₂O₃ and S incorporated Fe₂O₃.

	Pristine	Fe1	Fe2	Fe3	Fe4
Electron effective mass (m/m_e)	6.50	3.37	3.94	3.77	3.69

REFERENCES

- (1) Tamirat, A. G.; Su, W.-N.; Dubale, A. A.; Chena, H.-M.; Hwang, B.-J. Photoelectrochemical Water Splitting at Low Applied Potential Using a NiOOH Coated Codoped (Sn, Zr) α -Fe₂O₃ Photoanode. *J. Mater. Chem. A* **2015**, *3*, 5949–5961.
- (2) Huang, J.; Hu, G.; Ding, Y.; Pang, M.; Ma, B. Mn-Doping and NiFe Layered Double Hydroxide Coating: Effective Approaches to Enhancing the Performance of α -Fe₂O₃ in Photoelectrochemical Water Oxidation. *J. Catal.* **2016**, *340*, 261–269.
- (3) Cesar, I.; Kay, A.; Martinez, J. A. G.; Grätzel, M. Translucent Thin Film Fe₂O₃ Photoanodes for Efficient Water Splitting by Sunlight: Nanostructure-Directing Effect of Si-Doping. *J. Am. Chem. Soc.* **2006**, *128*, 4582–4583.
- (4) Li, N.; Jayaraman, S.; Tee, S. Y.; Kumar, P. S.; Lee, C. J. J.; Liew, S. L.; Chi, D.; Hor, T. S. A.; Ramakrishna, S.; Luo, H.-K. Effect of La-Doping on Optical Bandgap and Photoelectrochemical Performance of Hematite Nanostructures. *J. Mater. Chem. A* **2014**, *2*, 19290–19297.
- (5) Yan, D.; Tao, J.; Kisslinger, K.; Cen, J.; Wu, Q.; Orlovb, A.; Liu, M. The Role of the Domain Size and Titanium Dopant in Nanocrystalline Hematite Thin Films for Water Photolysis. *Nanoscale* **2015**, *7*, 18515–18523.
- (6) Annamalai, A.; Lee, H. H.; Choi, S. H.; Lee, S. Y.; Gracia-Espino, E.; Subramanian, A.; Park, J.; Kong, K.; Jang, J. S. Sn/Be Sequentially co-doped Hematite Photoanodes for Enhanced Photoelectrochemical Water Oxidation: Effect of Be²⁺ as co-dopant. *Sci. Rep.* **2016**, *6*, 28183.
- (7) Luo, Z.; Li, C.; Liu, S.; Wang, T.; Gong, J. Gradient Doping of Phosphorus in Fe₂O₃ Nanoarray Photoanodes for Enhanced Charge Separation. *Chem. Sci.* **2017**, *8*, 91–100.
- (8) Hu, Y.; Kleiman-Shwarstein, A.; Forman, A. J.; Dazen, D.; Park, J. N.; McFarland, E. W. Pt-Doped α -Fe₂O₃ Thin Films Active for Photoelectrochemical Water Splitting. *Chem. Mater.* **2008**, *20*, 3803–3805.

- (9) Liu, J.; Cai, Y. Y.; Tian, Z. F.; Ruan, G. S.; Ye, Y. X.; Liang, C. H.; Shao, G. S. Highly Oriented Ge-Doped Hematite Nanosheet Arrays for Photoelectrochemical Water Oxidation. *Nano Energy* **2014**, *9*, 282–290.
- (10) Sun, Y.; Chemelewski, W. D.; Berglund, S. P.; Li, C.; Shi, G.; Mullins, C. B. Antimony-Doped Tin Oxide Nanorods as a Transparent Conducting Electrode for Enhancing Photoelectrochemical Oxidation of Water by Hematite. *ACS Appl. Mater. Interfaces* **2014**, *6*, 5494–5499.